Green Fluorescent Protein Variants as Ratiometric Dual Emission pH Sensors. 2. Excited-State Dynamics†

Tim B. McAnaney,‡ Eun Sun Park,‡ George T. Hanson,§ S. James Remington,§ and Steven G. Boxer*,‡

Department of Chemistry, Stanford University, Stanford, California 94305-5080, and Departments of Chemistry and Physics and Institute of Molecular Biology, University of Oregon, Eugene, Oregon 97403-1229

Received August 9, 2002

ABSTRACT: In the preceding paper [Hanson, G. T., McAnaney, T. B., Park, E. S., Rendell, M. E. P., Yarbrough, D. K., Chu, S., Xi, L., Boxer, S. G., Montrose, M. H., and Remington, S. J. (2002) *Biochemistry 41,* 15477−15488], novel mutants of the green fluorescent protein (GFP) that exhibit dual steady-state emission properties were characterized structurally and discussed as potential intracellular pH probes. In this work, the excited-state dynamics of one of these new dual emission GFP variants, deGFP4 (C48S/S65T/H148C/T203C), is studied by ultrafast fluorescence upconversion spectroscopy. Following excitation of the high-energy absorption band centered at 398 nm and assigned to the neutral form of the chromophore, time-resolved emission was monitored from the excited state of both the neutral and intermediate anionic chromophores at both high and low pH and upon deuteration of exchangeable protons. The time-resolved emission dynamics and isotope effect appear to be very different from those of wild-type GFP [Chattoraj, M., King, B. A., Bublitz, G. U., and Boxer, S. G. (1996) *Proc. Natl. Acad. Sci. U.S.A. 93,* 8362−8367]; however, due to overlapping emission bands, the apparent difference can be analyzed quantitatively within the same framework used to describe GFP excited-state dynamics. The results indicate that the pH-sensitive steady-state emission characteristics of deGFP4 are a result of a pH-dependent modulation of the rate of excited-state proton transfer. At high pH, a rapid interconversion from the excited state of the higher energy neutral chromophore to the lower energy intermediate anionic chromophore is achieved by proton transfer. At low pH, excited-state proton transfer is slowed to the point where it is no longer rate limiting.

The green fluorescent protein (GFP)[1] from the jellyfish *Aequorea victoria* has become a ubiquitous tool in cell and molecular biology (*1*). The chromophore of wild-type GFP is formed spontaneously from the internal cyclization and oxidation of the Ser65-Tyr66-Gly67 tripeptide unit (*2*, *3*) and is protectively housed along a coaxial helix threaded through the center of an 11-stranded β-barrel (*4*). The surrounding protein environment is responsible for many of the emission properties of GFP such as the emission wavelength, relative contributions from neutral and anionic forms of the chromophores, and constraints that are responsible for the high fluorescence quantum yield. There has been a significant effort to change the surrounding environment by both random and semirational mutagenesis to produce GFP variants with desirable properties such as new emission wavelengths and improved quantum yields (*5*, *6*), more rapid chromophore maturation (*7*), greater structural stability (*8*, *9*), and altered sensitivity to environmental properties such as pH (*10*−*12*), redox potential (*13*), and ion concentration (*14*−*16*). In the preceding companion paper, a new class of pH-sensitive dual emission GFP (deGFP) mutants is reported (*17*). These mutants exhibit emission that changes from green (λ_{max} = 514 nm) to blue (λ_{max} = 465 nm) as the pH is lowered (Figure 1) and should be useful ratiometric pH sensors in vitro and in vivo. Structural studies of a related dual emission GFP, deGFP1 (S65T/H148G/T203C), show that while most of the wild-type GFP structure is preserved, the proton relay network near the chromophore observed in wild-type GFP does not appear to exist at either high or low pH.

At room temperature wild-type GFP exhibits two main absorption peaks with maxima at 398 nm (band A) and 478 nm (band B) and a single emission peak in the steady-state fluorescence spectrum around 510 nm. Previous studies have led to the assignment of these absorption bands to different protonation states of the chromophore, with the high-energy band corresponding to the neutral chromophore and the low-energy band to the anionic chromophore (*3*, *18*). Ultrafast proton transfer occurs in the excited state, leading to the formation of the deprotonated chromophore from which steady-state emission occurs, regardless of which band is excited. Scheme 1 shows a working model for the dominant photophysical processes of wild-type GFP at room temperature (*19*, *20*). Direct excitation of the anionic chromophore B results in green emission. Upon excitation of the neutral chromophore, A* rapidly converts to I*, an anionic chro-

† This work was supported in part by a grant from the NSF Biophysics Program. The fluorescence upconversion facilities are supported by the Medical Free Electron Laser Program of the Air Force Office of Scientific Research (Grant F49620-00-1-0349).

* To whom correspondence should be addressed. Tel: 650-723-4482. Fax: 650-723-4817. E-mail: sboxer@stanford.edu.

‡ Stanford University.

§ University of Oregon.

[1] Abbreviations: GFP, green fluorescent protein; ESPT, excited-state proton transfer; deGFP, dual emission green fluorescent protein; deGFP1, GFP variant (S65T/H148G/T203C); deGFP4, GFP variant (C48S/S65T/H148C/T203C); BFP, GFP variant (S65T/Y66H/Y145F) or blue fluorescent protein.

10.1021/bi026610o CCC: $22.00
Published on Web 12/07/2002

Scheme 1: Photophysics of Wild-Type GFP

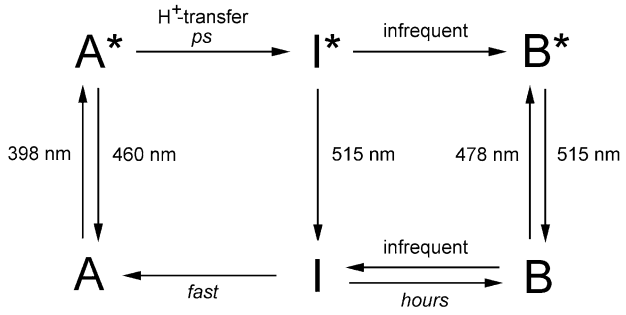

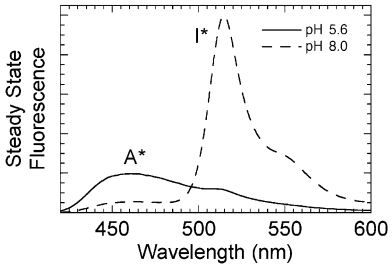

FIGURE 1: Steady-state fluorescence spectra of deGFP4 excited at 400 nm in pH 5.6 (solid line) and pH 8.0 (dashed line) buffers (*17*).

mophore similar to B* but in a nonequilibrium protein environment, and emits green fluorescence. The 460 nm emission from A* is only observed on a very short time scale, and its decay rate matches the rise of emission from I* measured at 510 nm. Both the A* decay and I* rise are slowed upon deuteration of exchangeable protons, which originally led to the suggestion that the process connecting these states is ultrafast excited-state proton transfer (ESPT) (*19*, *20*). The hydrogen bond network near the chromophore observed in the crystal structure of wild-type GFP is suggested to be responsible for ESPT (*21*). Although this scheme can account for many properties of wild-type GFP photophysics, it is surely incomplete (*22*−*26*). Nonetheless, it can provide a framework for interpreting results of GFP mutants, and it will be used as a working model for the analysis of the photophysical processes of deGFPs.

In this work, we investigate the excited-state dynamics of deGFP4 (C48S/S65T/H148C/T203C) by fluorescence upconversion spectroscopy. We examine the excited-state kinetics at both low and high pH and upon replacing exchangeable protons with deuterons to better understand the mechanism responsible for dual emission. The results are compared to wild-type GFP and BFP, a blue-emitting variant of GFP that does not undergo excited-state proton transfer (*20*, *27*). Even though the time-dependent emission appears to be very different from that of wild-type GFP, it is possible to model the data using the conventional scheme.

MATERIALS AND METHODS

Sample Preparation. Protein samples of deGFP4 were prepared as described in the companion paper (*17*). Samples of deGFP4 at pH 5.6 and 9.2, wild-type GFP at pH 7.2, and a BFP variant (S65T/Y66H/Y145F) at pH 8.0 in 50 mM buffer solutions (citrate, Tris, and HEPES as appropriate) were examined by fluorescence upconversion spectroscopy. For deGFP4 and wild-type GFP samples, exchangeable protons were replaced by deuterium by repeated dilution of the protein with the appropriate buffer in D_2O (buffers were not corrected for the isotope effect on the pH meter) and concentration to a minimal volume by ultracentrifugation (3×).

Fluorescence Upconversion Spectroscopy. The time evolution of fluorescence up to 160 ps at 460 and 515 nm was measured by a fluorescence upconversion setup described previously (*19*, *28*). Samples were excited with a 400 nm excitation pulse generated from the second harmonic of an argon ion pumped titanium−sapphire laser. The instrument response function generated from the mixing of the gate beam with the scattered excitation light was typically ∼170 fs. The sample, stirred continuously in a 1 mm path length quartz cuvette, was excited at 82 MHz with 10 mW of light polarized at the magic angle with respect to the gate beam (12 pJ/pulse).

Data Analysis. Data sets were fit to the convolution of the instrument response with a model function composed of a sum of exponentials, a baseline, and a time offset. Reported errors are the standard deviation of fit parameters from three data sets. The time-resolved emission of deGFP4 is not fit well by a single exponential; therefore, the average lifetime ($\langle\tau\rangle = \sum A_i\tau_i$) is also reported for convenience. Modeling of the 515 nm time-resolved emission as the sum of A* and I* kinetics used the fixed amplitudes and decay parameters from the 460 nm emission as the A* kinetics. The I* rise lifetimes were fixed to the A* decay lifetimes, and their respective amplitudes were varied to produce the best fit to the data. The I* decay lifetime was fixed to 2.8 ns, the value determined from time-correlated photon counting.

RESULTS

Excited-State Kinetics of deGFP4. To determine the basis for the pH-dependent steady-state emission properties of deGFPs (Figure 1), the early time fluorescence dynamics of deGFP4 were studied at both high and low pH and in protonated and deuterated buffer solutions. The excited-state dynamics were probed by exciting band A at 400 nm and monitoring the emission at 460 and 515 nm. For comparison, the emission from BFP and wild-type GFP was also measured. The results are shown in Figure 2, and the fit parameters for deGFP4 are summarized in Table 1.

The time-resolved emission of deGFP4 exhibits pH-dependent kinetics. At low pH, the emission at 460 nm decays with an average lifetime of 96 ps and is unchanged in deuterated buffer solution ($\langle t\rangle = 94$ ps). The emission at 515 nm is essentially identical to that measured at 460 nm with an average lifetime of 103 ps, but the decay kinetics become slightly faster upon replacing exchangeable protons with deuterons ($\langle t\rangle = 85$ ps). At high pH, the emission at 460 nm is rapidly quenched with an average decay lifetime of 35 ps and becomes slower in deuterated buffer ($\langle t\rangle = 55$ ps). The emission at 515 nm shows an initial ultrafast decay component with a lifetime of 4.2 ps comprising 14% of the total amplitude followed by long-lived emission (86%) that extends out well beyond our experimental time window (160 ps). Upon replacing exchangeable protons for deuterons, the decay of emission at 515 nm becomes substantially faster, with ultrafast decay components of 4.2 and 23 ps comprising a total of 54% of the total amplitude followed by long-lived emission (46%). Note that in no case does the fluorescence

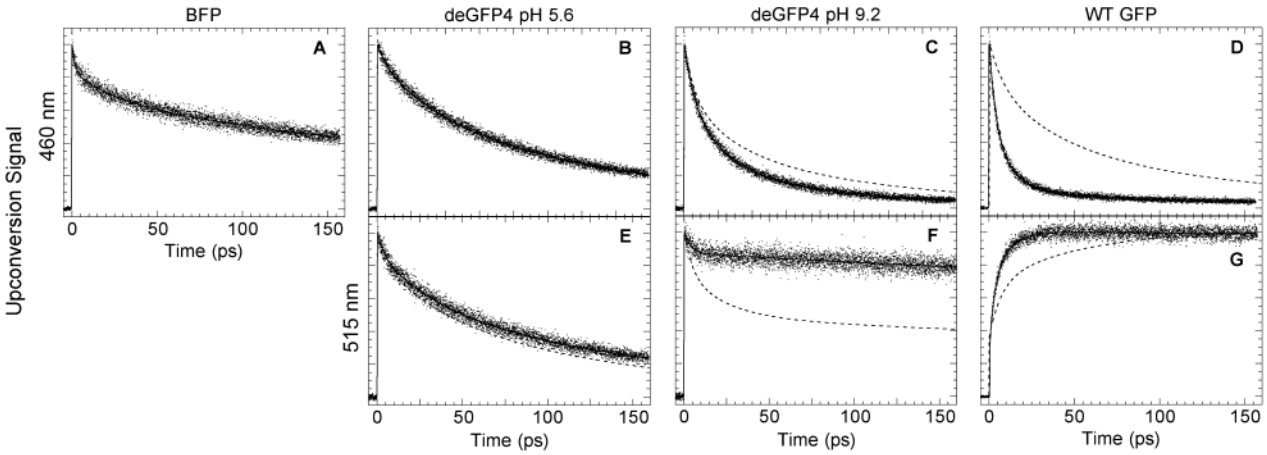

FIGURE 2: Time-resolved fluorescence of BFP, deGFP4 at pH 5.6 and 9.2, and wild-type GFP for excitation at 400 nm. Emission is shown (A−D) at 460 nm and (E−G) at 515 nm. Data (dots) and fits (solid line) are shown for BFP, deGFP4, and wild-type GFP; for clarity, deGFP4 and wild-type GFP data in deuterated buffers are omitted and only the fits (dashed line) are shown.

Table 1: Spontaneous Fluorescence Fit Parameters of deGFP4 Excited at 400 nm

		protonated buffer			deuterated buffer		
pH	λ_{em} (nm)	amp (%)[a]	τ (ps)	$\langle\tau\rangle$ (ps)[b]	amp (%)[a]	τ (ps)	$\langle\tau\rangle$ (ps)[b]
5.6	460	58 ± 3	146 ± 9	96	61 ± 5	135 ± 8	94
		32 ± 2	33 ± 4		32 ± 4	34 ± 6	
		10 ± 1	3.9 ± 1.0		7 ± 1	4.7 ± 1.8	
	515	54 ± 4	170 ± 11	103	56 ± 3	136 ± 1	85
		31 ± 3	34 ± 4		28 ± 2	29 ± 3	
		15 ± 2	3.1 ± 0.8		16 ± 2	3.1 ± 0.4	
9.2	460	20 ± 2	109 ± 7	35	38 ± 2	117 ± 4	55
		46 ± 1	25 ± 2		35 ± 1	25 ± 2	
		34 ± 2	5.9 ± 0.6		27 ± 3	5.3 ± 0.4	
	515	86 ± 5	≫160[c]	≫160[c]	46 ± 1	≫160[c]	≫160[c]
		14 ± 5	4.4 ± 2.7		30 ± 2	23 ± 1	
					24 ± 1	4.2 ± 0.4	
	I* model[d]	−3	109	23	−68	117	87
		−74	25		−29	25	
		−23	5.9		−3	5.3	

[a] Positive amplitudes indicate a decay time; negative amplitudes indicate a rise time. [b] The average lifetime $\langle\tau\rangle = \sum A_i\tau_i$. [c] Indicates a lifetime that is too long to be accurately measured with the 160 ps experimental time window. [d] The rise lifetimes of the intermediate anion kinetics were fixed to the decay lifetimes of the 460 nm emission.

rise outside the instrument response function for deGFP4 emission at either 460 or 515 nm.

DISCUSSION

Comparison of deGFP4 at Low pH to BFP. The steady-state emission spectrum of deGFP4 shows that excitation of band A at low pH produces a broad emission band at 460 nm that extends out beyond 515 nm (Figure 1). At low pH the decay kinetics measured at 460 and 515 nm are nearly identical, implying that the emission measured on the ultrafast time scale at either wavelength arises predominantly from the same excited-state species (Figure 2B,E). This response is similar to what is observed for BFP emission where nearly identical kinetics are measured as far out as 600 nm (*20*) and where the emission from A* is relatively long-lived (Figure 2A). The absence of both an appreciable deuterium isotope effect and a rise in the emission at 515 nm, features also absent in the emission from other BFP variants (*20*, *27*), indicates that efficient proton transfer does not occur on the time scale of the fluorescence lifetime of A* and that the emission at both wavelengths at low pH arises from A*. This behavior is also consistent with the structural data of the related dual emission variant which lacks a proton network near the chromophore in deGFP1 capable of ESPT (*17*). The slight isotope effect observed for emission at 515 nm will be discussed in further detail with the large isotope effect seen at high pH.

Comparison of deGFP4 at High pH to Wild-Type GFP. At high pH the emission band at 515 nm becomes more prominent in the steady-state fluorescence spectrum, and the emission at 460 nm becomes less intense (Figure 1). Comparison with the wild-type steady-state emission spectrum suggests that the dominant emission band observed at high pH arises from an intermediate anionic species (I*) formed through ESPT; however, the excited-state dynamics of deGFP4 at high pH appear to be completely different from those observed in wild-type GFP (Figure 2D,G). In wild-type GFP, excitation of band A results in an immediate emission at 460 nm from A*, which decays in a few picoseconds with a concomitant rise of green emission at 515 nm from I*. Both the decay of blue emission and the rise of green emission at 515 nm are slowed substantially upon deuteration, indicating that ESPT is involved in the conversion of A* to I* in wild type (*19*, *20*). The time-resolved emission of deGFP4 at 460 nm shows similar although slower picosecond decay kinetics compared to wild-

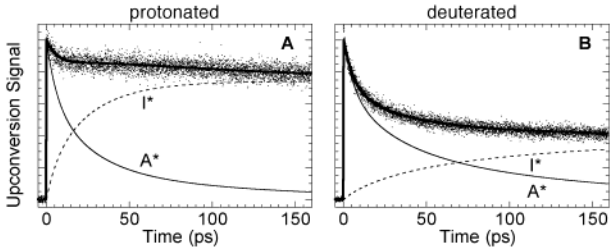

FIGURE 3: Decomposition of the time-resolved emission of deGFP4 at pH 9.2 into two populations. Emission at 515 nm is shown (A) in protonated buffer and (B) in deuterated buffer. A* kinetics (solid line) and I* kinetics (dashed line) are summed to obtain a fit (bold solid line) to the 515 nm emission data (dots). The A* kinetics are fixed to the fit of 460 nm emission and the I* population is modeled using the A* decay time constants as rise time constants (see text for details).

type GFP ($\langle t \rangle = 35$ and 25 ps respectively; Figure 2C,D). As is observed in wild-type GFP, the decay of emission at 460 nm is slowed upon replacing exchangeable protons with deuterons. The time-resolved emission of deGFP4 measured at 515 nm is completely different from that observed in wild-type GFP (Figure 2F,G). At 515 nm no rise kinetics are observed, and the decay of emission becomes *faster* in deuterated buffer solution.

The absence of a rise in the emission from the lower energy state and the negative isotope effect appear to be inconsistent with the scheme used to describe excited-state dynamics in wild-type GFP; however, there are some hints to the contrary. The isotope effect observed at 460 nm is analogous to that observed in wild-type GFP and is consistent with ESPT, though the emission at 515 nm lacks the distinctive kinetic characteristics associated with A* → I* conversion in wild type. The steady-state fluorescence spectrum is also significantly different from that of wild type. Appreciable steady-state fluorescence from A* is present at 460 nm (due to the longer A* lifetime), and given the broad shape of the A* emission band, it is likely that the emission bands associated with A* and I* overlap at wavelengths beyond 500 nm (Figure 1). This overlap should also be present in the time-resolved emission, and the kinetics observed at 515 nm could be a sum of the A* decay and I* rise kinetics. In the following, we show that, by taking this into account, the seemingly novel kinetics fit well with the model developed for wild-type GFP.

Modeling the 515 nm Emission as a Sum of A and I* Dynamics.* We model the time-resolved emission at 515 nm for deGFP4 at high pH as a sum of the emission from the neutral chromophore A* and the intermediate anionic chromophore I*. The A* decay kinetics at 515 nm are taken to be identical to those observed at 460 nm. The I* population that forms by ESPT from A* should exhibit rise kinetics identical to those of the A* decay kinetics. As described in Materials and Methods, we model the observed fluorescence kinetics at 515 nm as a linear combination of the measured A* decay and an I* population that rises with the A* decay lifetimes, with the only parameters being the relative amplitudes of the I* rise components. Figure 3 demonstrates that both the protonated and deuterated 515 nm emission can be accurately modeled in such a manner and that the relative contribution from the intermediate state decreases upon deuteration as is expected if A* → I* conversion is slowed. Table 1 summarizes the parameters used to model the kinetics of the intermediate anion. Decomposition of the time-resolved 515 nm emission into separate contributions from the A* decay and I* rise kinetics makes it apparent that ESPT is responsible for the predominantly green emission of deGFP4 at high pH. The A* and I* kinetic profiles extracted from this analysis now resemble those of wild type: both the decay of A* and the rise of I* occur on comparable picosecond time scales and slow upon deuteration. Further confirmation of this analysis is provided by the steady-state emission spectrum which exhibits a decrease in the 515 nm emission and concominant increase in the 460 nm emission upon replacing exchangeable protons with deuterons (data not shown). Although the high-pH structure of the related variant deGFP1 shows significant differences from wild type in the hydrogen bond network around the chromophore, our results indicate that the protein environment in the vicinity of the deGFP4 chromophore (and likely in the other deGFP variants) is still capable of ESPT, albeit with less efficiency than in wild type. The slower A* → I* ESPT results in a longer A* lifetime and emission that is readily detected in the steady-state fluorescence spectrum, thereby giving rise to the dual fluorescence.

The slight isotope effect seen at 515 nm at low pH can also be explained in such a manner, although the effect is much smaller than at high pH. The steady-state fluorescence spectrum shows a small contribution from I* at 515 nm (Figure 1), indicating that, even at low pH, a very small amount of ESPT occurs and produces a small population of I*. Upon deuteration, this process slows even further and results in a decrease in the contribution of I* kinetics to the time-resolved emission at 515 nm (because less I* is formed), resulting in a slightly faster decay lifetime. In the steady-state spectrum, the small contribution at 515 nm from I* emission decreases even further upon deuteration (data not shown).

Modeling the green emission as a sum of two distinct populations may be important for understanding the emission properties of other GFP mutants. Mutants which compromise the efficiency of excited-state proton transfer could result in increased blue emission and therefore detectable A* kinetics at longer wavelengths. For example, previous work by Lossau et al. on the F64L/S65T mutant revealed a lack of rise kinetics at 530 and 650 nm after excitation at 400 nm (*20*). The authors interpreted their results as a cancellation of picosecond rise and decay kinetics associated with I*; however, these picosecond decay processes did not appear upon direct excitation of the B band. It is possible that, upon excitation at 400 nm, emission at 530 and 600 nm is the sum of decaying A* emission and rising I* emission, similar to that observed here with deGFP4. The A* emission would be absent upon direct excitation of the low-energy B band, explaining why the picosecond decay components were not detected at 530 and 600 nm. Furthermore, Heikal et al. showed that the steady-state emission from A* at 450 nm is almost 30 times greater in F64L/S65T than in wild-type GFP (*29*), providing further evidence that such overlap issues may exist on the ultrafast time scale in the F64L/S65T mutant to a much greater extent than in wild type. It is therefore important to consider the possibility of emission from multiple states when drawing conclusions from time-resolved emission data. Even in cases where there is little or no evidence of emission from a particular species in the steady

Scheme 2: Schematic Diagram Combining the Structural Information of deGFP1 with the Photophysics of deGFP4[a]

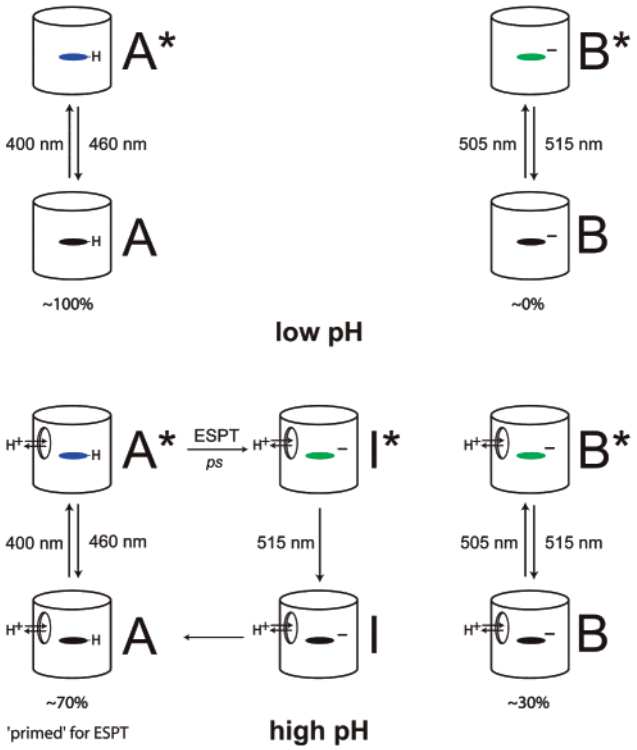

[a] Note that, at either pH, only one protein structure is present regardless of the chromophore protonation states. Upon excitation of the neutral chromophore at high pH, a proton relay network to the bulk solvent conducive to ESPT is present and results in green fluorescence from the anionic chromophore. At low pH, no proton relay network is present, and the neutral chromophore fluoresces blue. Direct excitation of the anionic chromophore B always results in green emission.

state, emission could be present and have a significant contribution on the ultrafast time scale.

Conclusions. The time-resolved emission of deGFP4 exhibits pH-dependent kinetics with novel dynamics observed at 515 nm. These interesting dynamics, the lack of rise kinetics and an apparent *negative* isotope effect, are consistent with the notion of pH-dependent, excited-state proton transfer when the time-resolved emission at 515 nm is treated as the sum of distinct A* and I* populations. The pH-dependent efficiency of proton transfer is most likely a result of the large structural changes accompanying pH modulation as inferred from the structural changes seen in deGFP1 (*17*). Scheme 2 depicts a general working model for deGFPs that combines the structural information of deGFP1 (*17*) and the excited-state dynamics of deGFP4. At high pH, the local chromophore environment includes a proton transfer relay to the bulk solvent that is capable of efficient ESPT and results in green emission from the anionic chromophore. Proton transfer becomes less efficient at acidic pH due to structural rearrangements that result in the loss of an adequate proton-transfer relay. The rate of ESPT can no longer effectively compete with other processes such as internal conversion back to the ground state (*30*), and emission is primarily from the neutral chromophore. At all pHs, A* → I* is slowed compared to wild-type GFP and results in the visible 460 nm steady-state fluorescence that makes deGFP4 a useful ratiometric pH sensor. However, in addition to their usefulness as pH sensors, deGFPs are

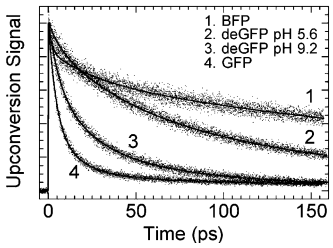

FIGURE 4: Comparison of the time-resolved fluorescence measured at 460 nm for (1) BFP, deGFP4 at (2) pH 5.6 and (3) pH 9.2, and (4) wild-type GFP for excitation at 400 nm.

excellent model proteins for experimental and theoretical study since their rates of ESPT can be systematically varied and controlled. To better visualize the dynamic range over which deGFP4 can modulate proton transfer, emission at 460 nm is compared in Figure 4 to that of wild-type GFP, which can be considered to exemplify efficient proton transfer (*19*, *20*), and a BFP variant, which serves as a model in the absence of proton transfer (*20*, *27*). When compared against these two limiting scenarios, deGFP4 is seen to modulate excited-state proton transfer over a fairly large range. Mutations that further stabilize the neutral chromophore in the excited state and increase the lifetime of blue emission would be desirable and improve the usefulness of deGFPs as ratiometric pH sensors.

ACKNOWLEDGMENT

We thank Federico Rosell for preparation of the wild-type GFP and BFP proteins and Jason Deich and W. E. Moerner for access to their time-correlated photon counting setup.

REFERENCES

1. Tsien, R. Y. (1998) *Annu. Rev. Biochem. 67*, 509−544.
2. Cody, C. W., Prasher, D. C., Westler, W. M., Prendergast, F. G., and Ward, W. W. (1993) *Biochemistry 32*, 1212−1218.
3. Heim, R., Prasher, D. C., and Tsien, R. Y. (1994) *Proc. Natl. Acad. Sci. U.S.A. 91*, 12501−12504.
4. Ormö, M., Cubitt, A. B., Kallio, K., Gross, L. A., Tsien, R. Y., and Remington, S. J. (1996) *Science 273*, 1392−1395.
5. Hein, R., and Tsien, R. Y. (1996) *Curr. Biol. 6*, 178−182.
6. Yang, T. T., Sinai, P., Green, G., Kitts, P. A., Chen, Y. T., Lybarger, L., Chervenak, R., Patterson, G. H., Piston, D. W., and Kain, S. R. (1998) *J. Biol. Chem. 273*, 8212−8216.
7. Heim, R., Cubitt, A. B., and Tsien, R. Y. (1995) *Nature 373*, 663−664.
8. Yokoe, H., and Meyer, T. (1996) *Nat. Biotechnol. 14*, 1252−1256.
9. Fukuda, H., Arai, M., and Kuwajima, K. (2000) *Biochemistry 39*, 12025−12032.
10. Kneen, M., Farinas, J., Li, Y. X., and Verkman, A. S. (1998) *Biophys. J. 74*, 1591−1599.
11. Miesenbock, G., DeAngelis, D. A., and Rothman, J. E. (1998) *Nature 394*, 192−195.
12. Elsliger, M. A., Wachter, R. M., Hanson, G. T., Kallio, K., and Remington, S. J. (1999) *Biochemistry 38*, 5296−5301.
13. Ostergaard, H., Henriksen, A., Hansen, F. G., and Winther, J. R. (2001) *EMBO J. 20*, 5853−5862.
14. Romoser, V. A., Hinkle, P. M., and Persechini, A. (1997) *J. Biol. Chem. 272*, 13270−13274.
15. Miyawaki, A., Llopis, J., Heim, R., McCaffery, J. M., Adams, J. A., Ikura, M., and Tsien, R. Y. (1997) *Nature 388*, 882−887.
16. Baubet, V., LeMouellic, H., Campbell, A. K., Lucas-Meunier, E., Fossier, P., and Brulet, P. (2000) *Proc. Natl. Acad. Sci. U.S.A. 97*, 7260−7265.
17. Hanson, G. T., McAnaney, T. B., Park, E. S., Rendell, M. E. P., Yarbrough, D. K., Chu, S., Xi, L., Boxer, S. G., Montrose, M. H., and Remington, S. J. (2001) *Biochemistry 41*, 15477−15488.
18. Cubitt, A. B., Heim, R., Adams, S. R., Boyd, A. E., Gross, L. A., and Tsien, R. Y. (1995) *Trends Biochem. Sci. 20*, 448−455.

19. Chattoraj, M., King, B. A., Bublitz, G. U., and Boxer, S. G. (1996) *Proc. Natl. Acad. Sci. U.S.A. 93*, 8362−8367.
20. Lossau, H., Kummer, A., Heinecke, R., Pollinger-Dammer, F., Kompa, C., Bieser, G., Jonsson, T., Silva, C. M., Yang, M. M., Youvan, D. C., and Michel-Beyerle, M. E. (1996) *Chem. Phys. 213*, 1−16.
21. Brejc, K., Sixma, T. K., Kitts, P. A., Kain, S. R., Tsien, R. Y., Ormo, M., and Remington, S. J. (1997) *Proc. Natl. Acad. Sci. U.S.A. 94*, 2306−2311.
22. Striker, G., Subramaniam, V., Seidel, C. A. M., and Volkmer, A. (1999) *J. Phys. Chem. B 103*, 8612−8617.
23. Weber, W., Helms, V., McCammon, J. A., and Langhoff, P. W. (1999) *Proc. Natl. Acad. Sci. U.S.A. 96*, 6177−6182.
24. Scharnagl, C., Raupp-Kossmann, R., and Fischer, S. F. (1999) *Biophys. J. 77*, 1839−1857.
25. Creemers, T. M. H., Lock, A. J., Subramaniam, V., Jovin, T. M., and Volker, S. (1999) *Nat. Struct. Biol. 6*, 557−560.
26. Cotlet, M., Hofkens, J., Maus, M., Gensch, T., Van der Auweraer, M., Michiels, J., Dirix, G., Van Guyse, M., Vanderleyden, J., Visser, A., and De Schryver, F. C. (2001) *J. Phys. Chem. B 105*, 4999−5006.
27. Wachter, R. M., King, B. A., Heim, R., Kallio, K., Tsien, R. Y., Boxer, S. G., and Remington, S. J. (1997) *Biochemistry 36*, 9759−9765.
28. Stanley, R. J., and Boxer, S. G. (1995) *J. Phys. Chem. 99*, 859−863.
29. Heikal, A. A., Hess, S. T., and Webb, W. W. (2001) *Chem. Phys. 274*, 37−55.
30. Kummer, A. D., Kompa, C., Lossau, H., Pollinger-Dammer, F., Michel-Beyerle, M. E., Silva, C. M., Bylina, E. J., Coleman, W. J., Yang, M. M., and Youvan, D. C. (1998) *Chem. Phys. 237*, 183−193.

BI026610O